ISBN: 978-3-95450-184-7 doi:10.18429/JACoW-IPAC2018-WEPML055

SIMULATION STUDY OF PARASITIC-MODE DAMPING METHODS FOR A 1.5-GHz TM020-MODE HARMONIC CAVITY

N. Yamamoto*, S. Sakanaka, T. Takahashi, KEK, Tsukuba, Ibaraki 305-0801, Japan

Abstract

Design study of parasitic-mode (PM) damped structures has been conducted for the purpose to realize a normal conducting 1.5 GHz harmonic cavity which is based on the TM020 resonant mode. We have investigated the performances of two PM-damping mechanisms, that are, rod-type antennas and annular slots. The rod-type antennas locate at the node of electric field of the TM020 mode while the annular slots locate at the node of magnetic field. As a result of 3D electromagnetic simulations, suitable performances of PMs were confirmed by employing either of the PM-damping mechanisms. It was also shown that the slot-type structure is superior in PM-damping performance and in the unloaded Q of the TM020 mode.

INTRODUCTION

A 1.5 GHz harmonic cavity based on the TM020 resonant mode is under design for an application of KEK light source (KEK-LS)[1, 2] and for the other quasi-diffraction-limited synchrotron radiation (SR) rings. For these rings, the longitudinal bunch lengthening by using a harmonic radio frequency (rf) system[3] is one of the solutions to mitigate the intrabeam scattering effect.

Recently, we reported the superiority of the TM020 harmonic cavity in the bunch lengthening performance due to it's high unloaded Q and small R/Q among existing normal conducting cavities at frequencies around 1.5 GHz[4]. Concerning to damp the parasitic-modes (PMs), which are lower and higher order modes other than the TM020-mode, the TM020 mode has the nodes of electric and magnetic fields at certain radial points, so that the PMs can be damped significantly while affecting little to the TM020-mode if we introduce the PM-damping mechanisms to these locations. Based on this concept, a novel damped accelerating cavity at a frequency 508.6 MHz was developed by Ego *et al.* by employing slot-type damping structures at the magnetic node[5].

Another damping mechanism using the electric node was proposed by the authors[6]. In [6], four rod-type antennas were inserted into the cavity from one of the side walls, which resulted in obtaining enough high external Q of the TM020-mode, that was, higher than 10^6. On the other hand, it was revealed that some PMs which have similar field shapes to the TM020 mode, such as the TM120 and TM021 modes, could not be damped well. This required additional ingenuities to perturb these PM fields.

We report in this paper the result of systematic investigations for both PM-damping mechanisms. We modeled PM-damped 1.5 GHz-TM020 cavities equipped with two different PM-damping mechanisms, and the performances were compared tentatively.

PARASITIC MODE OF TM020 CAVITY

In order to obtain the perspective on the PMs that should be damped, the resonant frequencies, unloaded Qs, and R/Qs were identified for a simple TM020 cavity without any additional ingenuities, such as nose-cones, round outer shapes, and damping mechanism. The numerical geometries of this cavity is summarized in Fig. I and Table I in [4]. An inner radius of the cavity was determined to tune the TM020 resonant frequency to be 1.500 GHz. The cavity has an R/Q of 77.2 Ω and an unloaded Q of 37,500.

The resonant frequencies and unloaded Qs of PMs, which were calculated below 3.5 GHz by CST MW studio[7], are summarized in Table 1; there are many dangerous PMs that should be damped. Although the parameters in Table 1 are affected by a modification of the cavity shape and by an introduction of PM-damped mechanism, Table 1 serves as a guideline of the PM properties.

For stable operation of the light sources, growth rates of the coupled bunch instabilities (CBIs) should be lower than the radiation damping rates of the beam. For the KEK-LS

Table 1: Calculated resonant frequencies and unloaded Qs of parasitic modes. The shunt impedance is defined by $R = V_c^2/P_c$.

Mode	Frequency [GHz]	UnloadedQ	R/Q [ΩΩ /m]
TM010	0.65	24560	167
TM110	1.04	30821	833
TM020	1.50	37238	76.9
TE111	1.65	28161	7.93
TM011	1.72	24083	6.1
TM111	1.89	25022	122
TM120	1.90	41104	447
TE121	2.13	48183	9.2
TM021	2.19	26991	33.8
TM030	2.35	46823	12.6
TM121	2.47	28164	513
TM130	2.75	48065	15.9
TE131	2.79	73110	3.3
TM031	2.85	30870	37.8
TM131	3.17	31301	514
TE112	3.19	36540	16.0
TM040	3.20	50705	0.1
TM022	3.24	33721	0.8
TM112	3.32	31767	51.6
TE122	3.46	44230	26.8

* naoto.yamamoto@kek.jp

ISBN: 978-3-95450-184-7 doi:10.18429/JACoW-IPAC2018-WEPML055

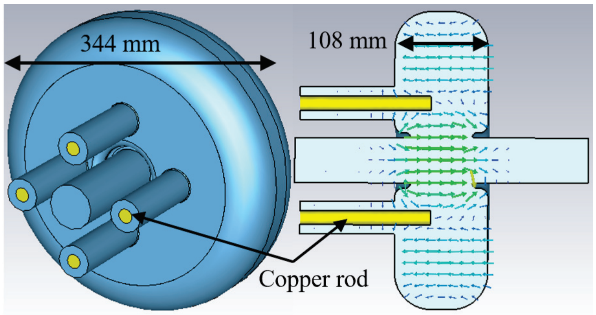

Figure 1: Perspective and cross views of the Rod-type structured damped-cavity. The electric field of TM020-mode are shown in cross view.

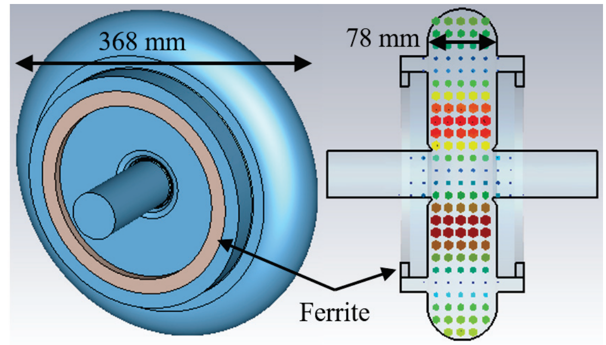

Figure 2: Perspective and cross views of the slot-type structured damped cavity. The magnetic field of TM020 mode are shown in cross view.

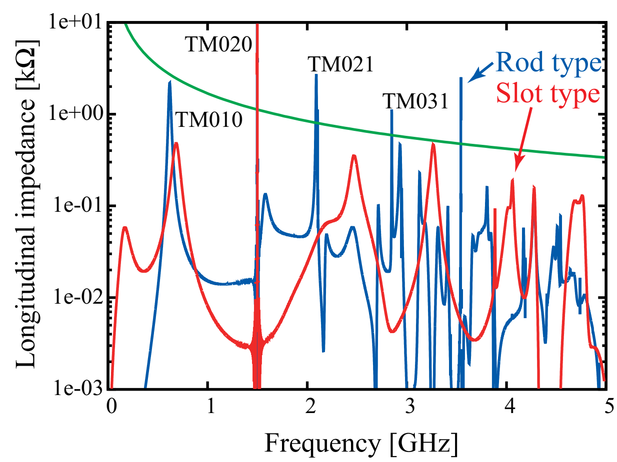

Figure 3: Longitudinal coupling impedance of the rod-type (blue) and the slot-type (red) damped cavities. The threshold impedance is also shown by a green curve.

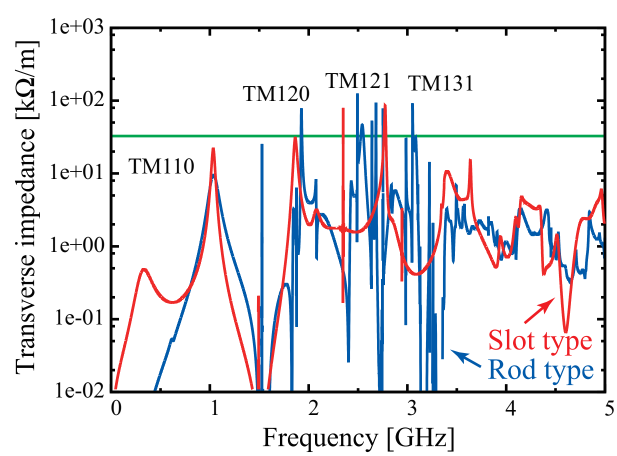

Figure 4: Transverse coupling impedance of the rod-type (blue) and the slot-type (red) damped cavities. The threshold impedance is also shown by a green line.

ring, the longitudinal threshold impedances were calculated to be a few kΩ for a frequency range of < 2 GHz, and 0.5 kΩ for ~ 3 GHz; the transverse threshold impedance is 33 kΩ/m. Note that we assumed the rigid bunch model with installing five TM020-mode harmonic cavities and only the contributions from the radiation losses in bending magnets were taken into account. Furthermore, the effect of the harmonic rf voltage on the CBIs were not included.

DESIGN OF TM020 DAMPED-CAVITY

Modeling the Damped-Cavity

We investigated two sorts of PM-damping mechanisms, that were, a) rod-type and b) slot-type mechanisms. The modeled cavities are shown in Figures 1 and 2. In both models, the beam pipe radius around 26 mm were chosen, and a cutoff frequency of the lowest mode corresponds to about 3.5 GHz.

Concerning the type a) in Fig. 1, four rod-type antennas were inserted into the cavity from one of the side walls. In this case, when the antennas locate at the electric node of the TM020 mode, fairly small degradation of the TM020 mode can be expected while strongly damping the PMs. The number of rods was chosen by considering the PM-powers extracted from the cavity, and these ports were assumed to be terminated by a characteristic impedance of 50 Ω in the calculation model. The external Q of these ports was around 1×10^9 for the TM020 mode.

For the type b) in Fig. 2, the annular slots were located at the magnetic node of the TM020 mode[5]. In this case, the PMs can strongly couple to these slots, and they can be damped by microwave absorbers that fit in the slots. We assumed to employ the ferrite (TDK, IB004) as microwave absorbers[8].

Calculation Results

The electromagnetic simulation code, CST MW studio[7], was employed for the estimation of the cavity performances. In our work, we optimized the resonant frequency and unloaded/external Q of the TM020 mode for each modeled cavity using the eigenmode solver, and then, we evaluated the coupling impedances for circulating beams using the wake field solver. The geometries of the cavity, such as nose-cones and outer round shapes, were iteratively modified to obtain better performances of coupling impedances.

ISBN: 978-3-95450-184-7 doi:10.18429/JACoW-IPAC2018-WEPML055

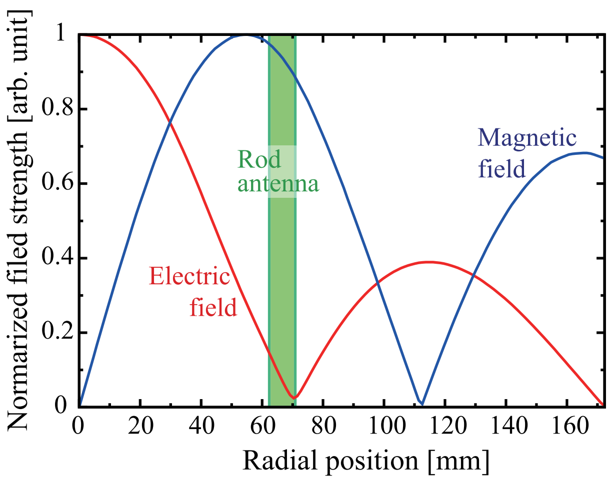

Figure 5: Normalized electric (red) and magnetic (blue) fields of TM020 mode as a function of the radial position.

Figure 3 shows our tentative results of the longitudinal impedances for both PM-damped structures. We also indicated the threshold impedances of the CBI described above as a green curve. For the slot-type structure shown by a red curve, it was found that the longitudinal impedance does not exceed the threshold over all calculation frequencies. In contrast, for the rod-type structure shown by a blue curve, we could not find a solution that meets the requirements yet; the impedance is at most higher than the threshold value by a factor of six.

For the transverse impedance shown in the Fig. 4, the calculated coupling impedances for both structures are higher than the threshold impedance by factors of four and two for the rod-type and slot-type structures, respectively.

Table 2 shows a summary of the calculated performances of the TM020 mode for both PM-damped structures. The unloaded Q of the rod-type structure was slightly smaller as compared to that of the slot-type structure. In the rod-type structure, the rod antennas were inserted at around the electric node of TM020-mode, where the magnetic field takes nearly its peak value, as shown in Fig. 5. Then we consider that the power loss of the TM020 mode is significantly large, and thus the unloaded Q is degraded. Quantitatively, the power loss on the surfaces of four antennas was estimated to be 9.6 % of total wall losses. This is consistent with the degradation of unloaded Q.

Table 2: Tentative performances of the TM020-mode of both damped cavities. The conductivity of the cavity material was assumed to be 5.8×10^7 S/m.

	Rod-type	Slot-type
Frequency [GHz]	1.500	1.500
R/Q [Ω]	72.5	70.5
Unloaded Q	29505	33575
External Q	1.03×10^9	-

DISCUSSION

As a result of our investigations, the slot-type mechanism seemed to be superior in the PM-damped performances and in unloaded Q of the TM020-mode. However, the differences are not critical; the cavity with the rod-type mechanism is also useful for such light source having larger radiation damping rates.

There are some advantages for the rod-type mechanism. Since coupling and absorbing functions for the PMs are separated, we can design these functions individually. The rod antennas can also be replaced easily in case of unexpected troubles.

Finally, we mention the coupled-bunch and single-bunch instabilities. There are many other factors affecting the CBI thresholds that were ignored in this paper. In case that insertion devices are fully installed to planned straight sections and they are operated with their minimum gaps, the radiation damping rates are increased by a factor of three at the KEK-LS. On the other hand, the harmonic rf voltage can affect significantly both coupled-bunch and single-bunch instabilities[9, 10]. Further investigation including these effects should be conducted hereafter.

CONCLUSION

Comparing the rod-type and the slot-type damped structures, about 10 % higher unloaded Q of the TM020 mode was obtained with the slot-type structure. The unloaded Q for the slot-type structure was estimated to be 33,575 with the R/Q of 70.5 Ω.

Concerning the coupling impedances for the lower and higher order modes, the slot-type structure showed better performances. The impedances of the slot-type structure were lower than the KEK-LS thresholds in longitudinal and two times higher in transverse. Considering expected increases in the damping rate due to insertion devices and/or an application of the transverse bunch by bunch feedback system, the transverse impedance is also considered to be acceptable.

As a next step, we started to design more practical cavities with an rf input coupler and frequency tuners. We also plan to conduct numerical calculations focused on the beam dynamics, such as single/coupled bunch instabilities and intrabeam effects, under harmonic rf operation.

ACKNOWLEDGEMENT

This work was supported by JSPS KAKENHI Grant Number JP17K05131.

ISBN: 978-3-95450-184-7 doi:10.18429/JACoW-IPAC2018-WEPML055

REFERENCES

[1] K. Harada et al., "The HMBA lattice optimization for the new 3 GeV light source," in *Proc. 7th Int. Particle Accelerator Conf. (IPAC'16)*, Busan, Korea, Jun. 2016, pp. 3251–3253, doi: 10.18429/JACoWIPAC2016-THPMB012

[2] T. Honda, "Concept of a new generation synchrotron radiation facility KEK Light Source," in *Proc. 8th Int. Particle Accelerator Conf. (IPAC'17)*, Copenhagen, Denmark, May 2017, pp. 2687–2690, doi: 10.18429/JACoW-IPAC2017-WEPAB047

[3] [A. Hofmann and S. Myers, "Beam dynamics in a double rf system," in *Proc. 11th Int. Conf. on High-Energy Accelerators*, CERN-ISR-TH-RF-80-26, , pp. 610–614, Springer, 1980.

[4] N. Yamamoto, T. Takahashi, and S. Sakanaka, "Reduction and compensation of the transient beam loading effect in a double rf system of synchrotron light sources", *Phys. Rev. Accel. Beams*, vol. 21, no.1, p.012001, Jan. 2018, doi: 10.1103/ PhysRevAccelBeams.21.012001

[5] H. Ego, J. Watanabe, S. Kimura, and K. Sato, "Design of a HOM-damped rf cavity for the SPring-8-II storage ring", in *Proc. 11th Annual Meeting of Particle Accelerator Society of Japan*, paper MOOL14 [in Japanese], PASJ, Tokyo, 2014, pp. 237–241.

[6] T. Takahashi, S. Sakanaka, and N. Yamamoto, "Design study of damped accelerating cavity based on the TM020-mode and HOM couplers for the KEK Light Source project", in *Proc. 8th Int. Particle Accelerator Conf. (IPAC'17)*, Copenhagen, Denmark, May 2017, pp. 4172–4175, doi: 10 . 18429 / JACoW - IPAC2017 - THPIK036

[7] D. Systèmes, CST Microwave Studio. `http://www.cst.com`

[8] Y. Suetsugu, T. Ishibashi, H. Ishizaki, A. Kimura, T. Sawhata, and S. Terui, "Fabrication of ferrite-copper block by Spark Plasma Sintering (SPS)," in *Proc. 7th Int. Particle Accelerator Conf. (IPAC'16)*, Busan, Korea, May 2016, pp. 3654–3656, doi: 10.18429 / JACoW - IPAC2016-THPMY002

[9] M. Venturini, "Harmonic cavities and the transverse modecoupling instability driven by a resistive wall", *Phys. Rev. Accel. Beams*, vol. 21, p. 024402, Feb. 2018, doi:10.1103/PhysRevAccelBeams.21.024402

[10] R. Lindberg, "Theory of longitudinal multibunch instabilities including a higher-harmonic (bunch-lengthening) cavity", in *Proc. Future Light Source workshop. (FLS'18)*, Shanghai, China, Mar. 2018, paper THP1WB03.